Moisture Transfer and Drying Stress of *Eucalyptus* Wood during Supercritical CO_2 ($ScCO_2$) Dewatering and $ScCO_2$ Combined Oven Drying

Honghai Liu,[a,b,]* Jinge Xie,[a] and Jingwen Zhang [a]

Supercritical CO_2 ($ScCO_2$) dewatering is a lumen water expulsion process, in which CO_2 is cycled between atmospheric pressure and supercritical phase and results in a fast expulsion of free water. In this study, specimens of 100 mm length *Eucalyptus exserta* F.V. Muell. wood were dewatered using $ScCO_2$, then the dewatered and un-dewatered wood were dried in oven at 100 °C to investigate moisture transfer and drying stress. The $ScCO_2$ dewatering was very fast. When the moisture content (MC) was over 40%, the MC distribution and gradient after dewatering and oven drying were different. The oven drying MC showed a ring contour distribution, but the $ScCO_2$ showed a higher MC in one side and a lower MC in the opposite; the oven drying MC gradient was great in the middle and small in the end part of wood, but the $ScCO_2$ MC gradient was small and roughly consistent. The oven drying moisture migration rates along the fiber and transverse directions were similar; however, the $ScCO_2$ migration rate was faster in the transverse directions. The MC distributions of the dewatered and un-dewatered wood after oven drying were similar at 30% MC. The $ScCO_2$ dewatering reduced wood residual stress, and it affected the stress development in the subsequent oven drying.

DOI: 10.15376/biores.17.3.5116-5128

Keywords: Eucalyptus; Supercritical CO_2 dewatering; Oven drying; Moisture distribution; Moisture transfer

Contact information: a: College of Furnishings and Industrial Design, Nanjing Forestry University, Nanjing 210037 China; b: Jiangsu Co-Innovation Center of Efficient Processing and Utilization of Forest Resources, Nanjing Forestry University, Nanjing 210037, China;
** Corresponding author: liuhonghai2020@njfu.edu.cn*

INTRODUCTION

Eucalyptus plantations are widely planted in the southern regions of China due to their strong environmental adaptability and fast growth rate. They are the important industrial raw materials for the paper, wood-based panels, and fiber industries (Yang *et al*. 2022; Morales *et al*. 2017; Carignato *et al*. 2018; Zhen *et al*. 2021). There are some plantation eucalyptus species that have higher mechanical properties and beautiful grains; these have potential for use in high value-added solid wood products, such as furniture, flooring, doors, and windows (Teixeira *et al*. 2009; Chen and Zhu 2019; Zhao *et al*. 2021; Zhang *et al*. 2021; Yang and Jin 2021; Ruben *et al*. 2021). However, most plantation eucalyptus woods are prone to collapse and deformation during conventional kiln drying (CKD), and special drying conditions or processing is necessary for their further application (Wingate-Hill and Cunningham 1986; Franich *et al*. 2020; Huang *et al*. 2020).

Supercritical CO_2 ($ScCO_2$) dewatering has great potential in the difficult-to-dry wood due to its good solubility, strong transfer capacity, and special dewatering mechanism (Todd and Baroutian 2017; Ferrentino *et al*. 2018). However, eucalyptus experiences collapse and deformation during CKD because of its poor wood permeability. The capillary tension caused by free water migration in the CKD process applies pressure to the cell wall of wood, and cells collapse when the capillary tension is greater than their compressive limit (Tiemann 1941). To reduce the collapse in CKD, microwave (Zhou *et al.* 2009), compression (Hayashi and Terazawa 1975), and pre-freezing (Zhang *et al*. 2011) treatments are used before drying (Zuo *et al*. 2016), but the collapse cannot be solved completely. There are several dewatering methods that eliminate liquid capillary tension and solve the collapse and deformation of wood cells radically (Franich *et al*. 2014; Dawson *et al*. 2020).

The dewatering method of $ScCO_2$ is proposed for difficult-to-dry wood to shorten the drying time and reduce the deformation. During the dewatering process, the CO_2 is cycled in the equipment between supercritical and gas phase through changing the pressure. The $ScCO_2$ has excellent heat and mass transfer properties, and it can penetrate easily into wood. The $ScCO_2$ turns into CO_2 gas phase by reducing the pressure, which expels the free water out of wood (Dawson *et al*. 2015; Gabitov *et al*. 2017; Dawson *et al*. 2017). Studies have shown that the water in wood is removed at concentrations much higher than its solubility limit in $SuCO_2$, which implies that $ScCO_2$ mechanically displaces some of the water from the wood structure (Aggarwal *et al*. 2019; Banerjee *et al*. 2022). This dewatering can result in very small negative capillary tension and prevent wood collapse (Zhang *et al*. 2019; Yang 2021).

The $ScCO_2$ dewatering method has a higher dewatering rate and less deformation, but it can only dewater wood to near the fiber saturation point (FSP) (Dawson *et al*. 2015, 2020). Behr *et al*. (2014) and Meder *et al*. (2015) have studied the water distribution of wood after $ScCO_2$ dewatering, but they did not analyze the characteristics of water distribution and transfer in wood fiber direction. Meanwhile, there were some discussions on the practical application of $ScCO_2$ dewatering. Aggarwal *et al*. (2019) pointed out that $ScCO_2$ dewatering for pine flakes is potentially much more cost-effective than thermal drying from both capital and operational perspectives. The dewatering test for commercial potential with green radiata pine wood specimens (100×50×300 mm) using large-diameter pressure vessels and ancillary machinery has successfully performed (Dawson *et al*. 2020). The test showed the same results as those obtained from using the larger laboratory specimens. However, a significant benefit for wood product manufacture may be the ability to sequentially dewater green wood and then undertake wood modification (Franich *et al*. 2020).

In the current study, *Eucalyptus exserta* F.V. Muell. samples were first dewatered to 40% moisture content (MC) using $ScCO_2$, and the dewatered and un-dewatered samples were dried to 30% MC in an oven at 100 °C. The dewatering rate, MC distribution in the middle and the end of the wood, the characteristics of MC transfer, and the drying stress of wood in the $ScCO_2$ dewatering, oven drying, and $ScCO_2$ dewatering combined with oven drying were compared.

EXPERIMENTAL

Materials

Eucalyptus exserta F.V. Muell. trees were collected from Guangxi, China. Their diameter at the collection height was approximately 200 mm. The trees were prepared into logs with 1000 mm length, and subsequently, they were prepared into lumbers with dimensions of 30(R) × 30(T) × 1000(L) mm, sealed using plastic films, and stored at 4 °C. Two lumber pieces were sawed into end-matched samples (8 pieces) with dimensions of 30(R) × 30(T) × 100(L) mm, as illustrated in Fig. 1. The average initial MC of all samples was 58%.

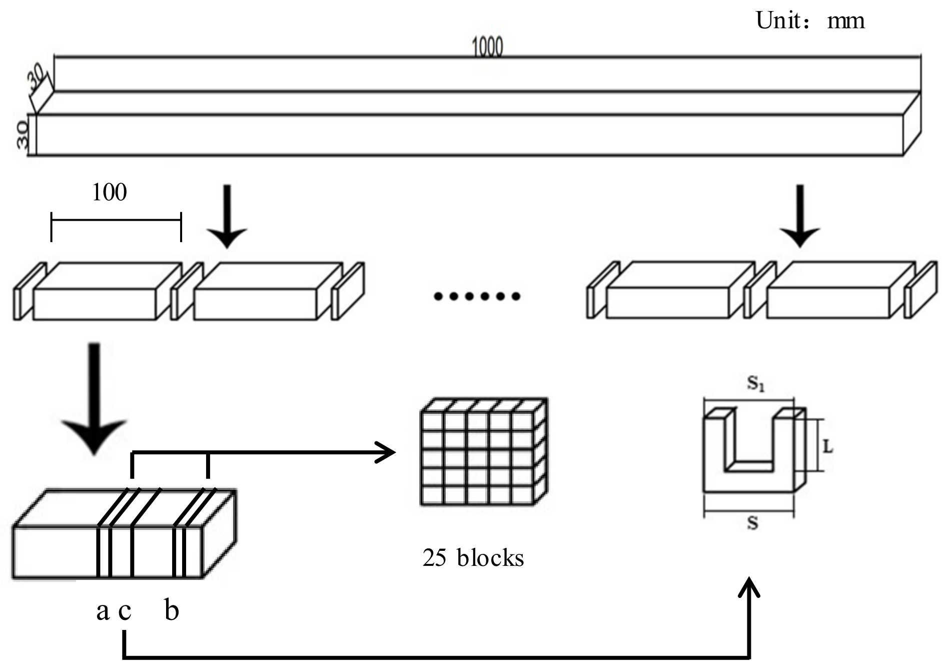

Fig. 1. Diagram of sample preparation

Equipment

The drying devices include a $ScCO_2$ dewatering equipment (DY221-50-06; Huaan Supercritical Fluid Extraction Co., Ltd, Nantong, Jiangsu, China), an electricity heating oven (DHG-905386-III, Shanghai Cimo Medical Instrument Co., Ltd, Shanghai, China), an electronic balance, HC2004 (0.001g, Sincere Dedication of Science and Technology Innovation Company, Shanghai, China), and an electronic vernier caliper (CD-20CPX (0.01mm, Mitutoyo Co., Ltd., Tokyo, Japan).

Wood $ScCO_2$ Dewatering

Wood $ScCO_2$ dewatering tests were conducted according to the parameters in Table 1, which was obtained based on the trial test. The drying procedures are illustrated in Fig. 2). The process included the following: 1) opening the sealing valve of the drying vessels, inserting samples into the vessels and then closing the sealing valve; 2) setting the drying temperature at 45 °C and starting the heating device; 3) opening the valve of CO_2 bottle, transferring CO_2 to drying vessels (Fig. 2-3,4), then increasing the temperature and pressure of CO_2 to supercritical stage (45 °C/25 MPa); 4) $ScCO_2$ penetrating into wood and dissolving water in the drying vessels, and then delivering water to adsorption vessels (Fig. 2-5,6) by lowing the pressure of $ScCO_2$; 5) 15 min later, decreasing temperature and pressure of $ScCO_2$, taking out samples as pressure reaching to atmosphere pressure; 6) samples were kept in room temperature for 30 min to release CO_2 in wood, then were measured on a balance. This completed one full drying cycle. Several drying cycles were performed to decrease the MC of wood to 40%, and then the mass of samples was measured again. A total of 8 samples were dewatered, 4 of them were sawed and prepared for determination of MC distribution and stress, and the remaining 4 samples were oven-dried.

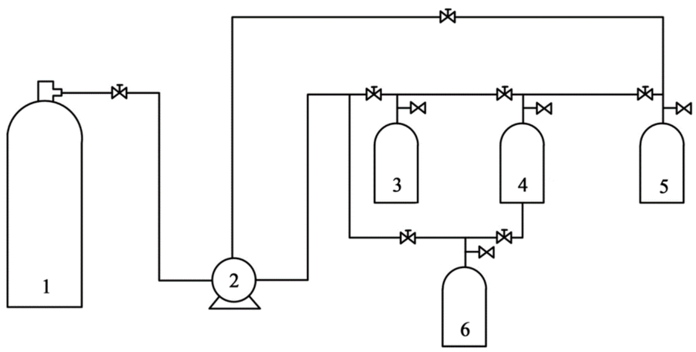

Fig. 2. Schematic diagram of the equipment and $ScCO_2$ dewatering process. (1) CO_2 bottle; (2) pump; (3, 4) drying vessel; (5, 6) drying adsorption vessel

Table 1. Parameters of Supercritical CO_2 Dewatering

Parameters	Values
Maximum pressure (MPa)	25
Minimum pressure (MPa)	0.1(atmospheric pressure)
Pressure rise time (min)	30
Decompression time (min)	10
Drying temperature (°C)	45
Hold time (min)	15

$ScCO_2$ Dewatering Combined with Oven Drying and Oven Drying

After the dewatering tests, 4 dewatered samples together with the 8 un-dewatered samples were oven-dried (OD) at 100 °C. The combined drying is termed as $ScCO_2$-Oven. During oven drying, all samples were tanked out in 10-min intervals and cooled in sealed bags, then were measured for mass using an electronic balance and dimensions with an electronic vernier caliper. They were oven dried until their MCs decreased to 30%.

Determination of Moisture Content and Moisture Distribution

The MC of the samples was determined in accordance with GB/T 1931 (2009). When the MC of wood decreased to 40 and 30% during dewatering or oven drying, thin slices were sawn in the middle (Fig. 1a) and the right end (Fig. 1b) of three samples. A thin slice was immediately split into 25 small blocks (Zhou *et al.* 2009; Gabitov *et al.* 2017), which were dried in an oven at 103 ± 2 °C to obtain their MCs (Meder *et al.* 2015). The

MC distribution charts were plotted using the data of three samples and Origin 2021 software (OriginLab Corporation, Northampton, USA).

Residual Stress Determination

The residual stress was determined according to GB/T 6491 (2012). After the oven drying, a 10-mm-thick sample (Fig. 1c) was sawn from a sample and then dried in an oven at 103 ± 2 °C for 2 h, which produced a stress sample with a concave shape as shown in Fig. 1. The initial dimensions of S and L were measured using an electronic digital caliper, and then it was placed in a ventilated place at room temperature for 24 h. The final dimension of S_1 was measured using an electronic digital caliper. The residual stress index Y was calculated using Eq. 1, which was the average values of four stress samples,

$$Y = (S - S_1)/2L \tag{1}$$

where Y is the residual stress index (%), S is the initial width of the stress sample (mm), S_1 is the final width of the stress sample (mm), and L is the length of the stress sample (mm).

RESULTS AND DISCUSSION

Drying Curves of ScCO$_2$-Oven and OD

Figure 3 shows the curves of combined process of ScCO$_2$-Oven and OD alone. The MC decreased from 58% to 39% in 1 h in OD process, while, it took 1.5 h until the MC decreased to 36% in ScCO$_2$ dewatering process. The drying rate of OD was faster because the water in wood was converted into steam at 100 °C. Compared with the curves of ScCO$_2$ dewatering to OD in Fig. 3, the ScCO$_2$ dewatering rate was 73% of OD, indicating a fast dewatering.

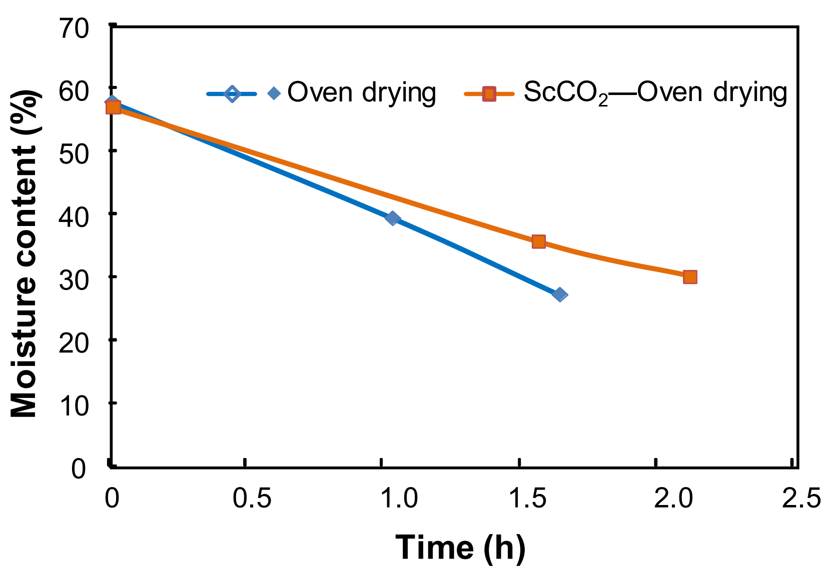

Fig. 3. Moisture change curves of oven drying and ScCO$_2$-oven drying

In contrast to previous conventional kiln drying with the same sample size performed at 50 °C and 84% relative humidity (Zhang *et al*. 2020), the dewatering rate of $ScCO_2$ was 2.5 times higher. Therefore, $ScCO_2$ has a very fast dewatering rate when the MC is above 40%. When the MC decreased from 40 to 30%, the drying rate of OD alone increased a little, while samples after $ScCO_2$ dewatering decreased in this period. The early $ScCO_2$ dewatering results in low initial temperature (45 °C) of wood and different MC gradients (Fig. 4), leading to a relative low drying rate in the subsequent oven drying. Furthermore, the $ScCO_2$ dewatering opened up the pore openings within the wood. The improved permeability of wood is beneficial for water removal and modifier penetration in the subsequent treatments, such as drying and impregnation modification (Newman *et al*. 2016; Yang and Liu 2020; Xu *et al*. 2021; Yang *et al.* 2021; Cao *et al*. 2021; Pang *et al*. 2021).

MC Distribution in Wood after Oven Drying and $ScCO_2$-Oven

Figure 4 shows a two-dimensional distribution MC in the middle (Fig. 4a) and in the end (Fig. 4b) of the wood, when the MCs were at initial, 40 and 30% stages for $ScCO_2$-Oven and oven alone. Figure 5 is the average MC of the wood blocks (Fig. 1a, b) and their standard deviations (error bars) at the corresponding MC stages.

The initial MC of samples used for two dryings tests are uniform, showing a similar average MCs and error bars (Fig. 5). When the MC decreased to 40%, the distribution of MC of wood after $ScCO_2$-Oven and oven alone were different. The MC of wood after oven drying presented a ring contour distribution, showing a higher MC in central and lower MC outside (Fig. 4a, b). The contour in the middle of the sample was crowded, but become thin in the end of the sample. This result indicated a greater MC gradient in the middle and a smaller gradient in the end. A similar phenomenon was found in Fig. 5a, b. The error bars of the average MC in the middle of the sample were much larger than those in the end, indicating a bigger MC gradient in the middle of the sample. However, the MC of wood after dewatering showed a higher MC distribution in one side and a lower MC in the opposite side (Fig. 4a, b). Whether in the middle or the end of the samples, the MC contour was gently transitioned from one side to the opposite side, showing a small and roughly consistent MC gradient. The error bars of the sample in the middle and in the end after dewatering were similar, indicating that the MC distribution and difference were quite small.

When the MC decreased from 40% to 30%, all samples underwent oven drying. Thus, the MC of the samples showed a similar tendency, *i.e*., a higher MC distribution in one side and a lower MC in the opposite side. The MC distribution of oven drying alone was similar in the middle and in the end of sample, but the error bars in the middle were greater than that in the end (Fig. 5a, b.), indicating a higher MC gradient in the middle. The errors of MC in the end of samples (Fig. 5a, b.) after $ScCO_2$ dewatering were greater than the middle, showing a higher MC gradient in the end. This result could be attributed to the effect of $ScCO_2$ dewatering to wood (Franich *et al*. 2014).

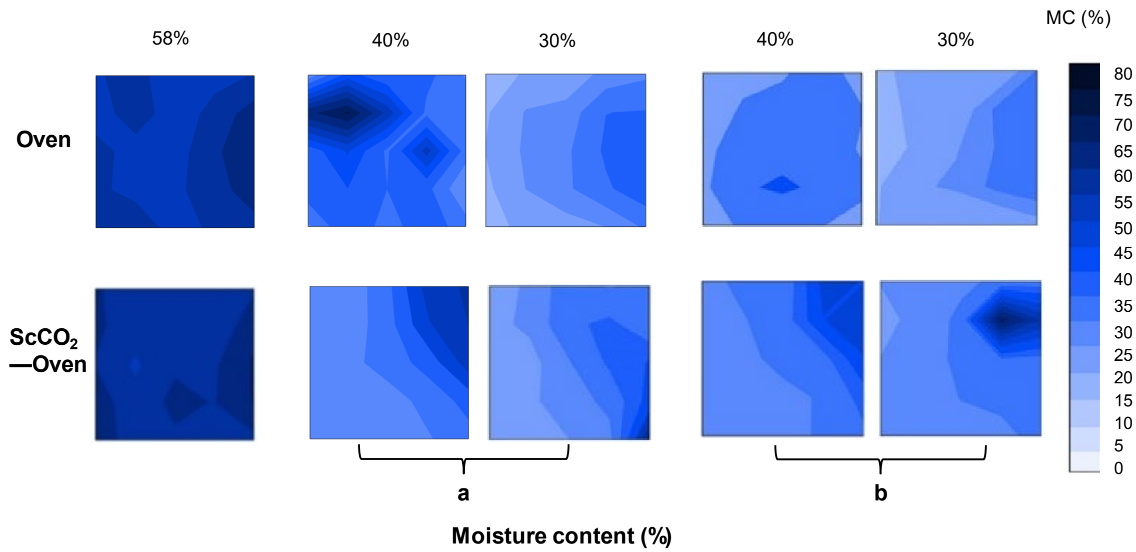

Fig. 4. Moisture distributions in wood during drying. a: middle of sample and b: end of sample

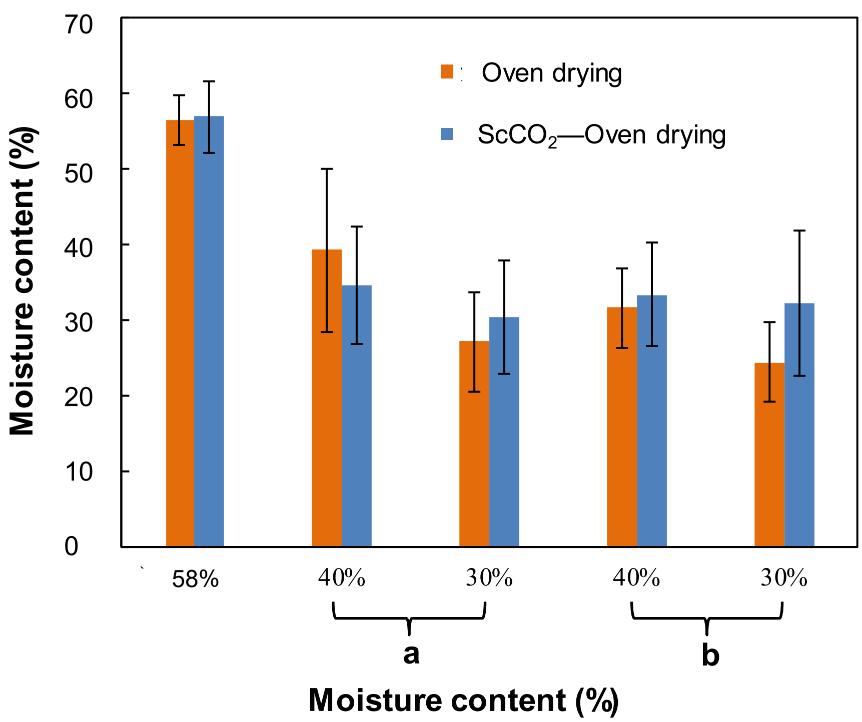

Fig. 5. Moisture content and its deviation of MC samples. a: middle of sample and b: end of sample. Bars indicate the standard deviations for the wood blocks cut from each sample.

Characteristics of Moisture Transfer in Wood during Drying

Figure 6 shows the MC gradients in wood fiber and transverse direction (perpendicular to the fiber direction) when the MCs were at 40 and 30% for $ScCO_2$-Oven and oven alone. The characteristics of moisture transfer during drying were studied based on the MC distributions in Fig. 4 and the MC gradients in Fig. 6. When the MC was 40%, the gradients of oven drying alone in fiber direction were approximately 8.3%, which are largely similar to those in the middle and end. This result indicates that the moisture transfer in fiber and transverse direction were almost same, showing a very fast moisture migration. As the MC decreased to 30%, the MC gradients decreased to an average value of 3.4%, but with obvious differences. The MC gradient in the transverse direction in the middle was the greatest, followed by the end, and the lowest value was in the fiber direction. The MC gradient in the transverse direction was 1.4 times that in fiber direction, indicating that MC migration occurred mainly along the transverse direction in this stage.

The MC gradient variation of the $ScCO_2$-Oven drying was different from oven drying alone. When the MC was 40%, the MC gradient had a positive value, indicating that the MC in the middle was greater than the end. However, the MC gradients in the middle and end were both negative values, indicating that wood in the central MC was lower than wood surface. This result indicates that wood central moisture migrated to the end and the side surfaces of wood simultaneously, but the migration rate in transverse direction was greater than the fiber direction. As the MC decreased to 30%, the MC gradient value in fiber direction became negative, indicating the MC in the end was greater than the central part. In this stage, the MC gradient value in the middle of sample was still negative, but became much smaller than that at 40% MC. However, the MC gradient value in the end became positive, indicating the MC in the central part in the end of sample was greater than at the surfaces part. This data indicated that subsequent oven drying affected the MC distribution of wood dewatered by $ScCO_2$, which resulted in a fast transverse migration of water in the surface parts in the middle and end of samples.

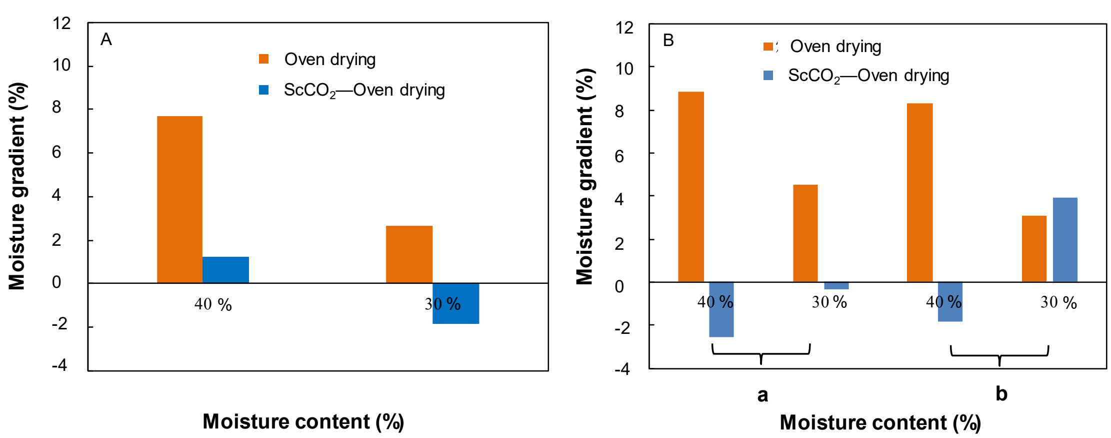

Fig. 6. Moisture content gradients in fiber direction (A) and transverse direction (B) of the samples. a: middle of sample and b: end of sample

Residual Stress of Wood after Drying

Figure 7 presents the residual stress in wood when the MCs were at 40 and 30% stages for $ScCO_2$-Oven and oven alone. The residual stress of oven drying alone was higher than $ScCO_2$ dewatered along and $ScCO_2$-Oven drying when the MC was close to 30%. This result indicates $ScCO_2$ dewatering can reduce the residual stress, but it affects the stress development in the subsequent oven drying. The reason may due to the effect of $ScCO_2$ dewatering on the MC distribution in wood, which influences the shrinkage and stress when the MC of wood was lower than fiber saturated point (FSP). Furthermore, the microstructure of wood was modified by early $ScCO_2$ dewatering (Newman *et al*. 2016), which affects the moisture migration, shrinkage, and stress development in the subsequent oven drying. When the MC was 40%, the residual stress was 5%, indicating $ScCO_2$ dewatering also can result in stress at high MC stages. It can be explained by the MC distribution in Fig. 4. In this stage, the average MC was about 40%, but the MC distribution was uneven. The MC of samples in certain locations was also lower than FSP, where wood has begun to shrink (Yang *et al.* 2020), leading to stress. The residual stress between $ScCO_2$-oven and oven alone was not clearly significant when the MC dropped to 20%, indicating the effect of $ScCO_2$ dewatering on transfer and distribution of moisture were progressively weaker, and oven drying controlled the development of the stress.

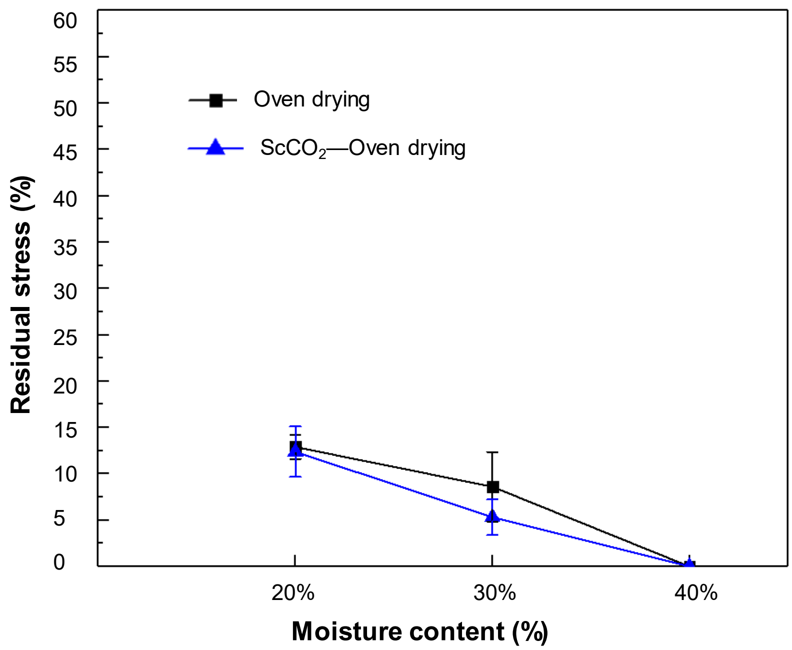

Fig. 7. Residual stress of oven drying and $ScCO_2$-oven at various MC stages

CONCLUSIONS

1. When the moisture content (MC) was above 40%, the drying rate with supercritical carbon dioxide ($ScCO_2$) was very fast, *i.e.* 73% and 2.5 times of that in oven and conventional kiln drying, respectively. The drying rate of $ScCO_2$-O was less than the oven drying.
2. When the MC was above 40%, the MC distributions of $ScCO_2$ dewatering and oven drying were different. The MC of oven drying showed a ring contour distribution with a higher MC in the center and lower MC outside. The MC gradient was great in the middle and small in the end part of wood. However, the $ScCO_2$ dewatering showed a higher MC distribution in one side and a lower MC in the opposite side. The MC gradient in the middle and the end of wood was small and roughly consistent. The

moisture migration rate along the fiber and transverse directions in the oven drying was roughly same; however, it was faster in the transverse directions in the $ScCO_2$ dewatering.

3. When the MC decreased to 30%, the MC distribution of dewatered and un-dewatered wood after oven drying was similar, showing a higher MC in one side and a lower MC in the opposite side. The moisture migration in oven drying was mainly along transverse direction.
4. At all MC stages, the residual stresses in the oven were greater than $ScCO_2$ dewatering and $ScCO_2$-Oven drying. The $ScCO_2$ dewatering reduced the residual stress of wood, and affected the stress development in the subsequent oven drying.

ACKNOWLEDGMENTS

The authors are grateful for the support of the National Natural Science Foundation of China (Grant Nos. 31870545 and 31570558) and Nanjing Forestry University Undergraduate Innovation Training Project (2021NFUSPITP0700).

REFERENCES CITED

Aggarwal, S., Johnson, S., and Hakovirta, M. (2019). "Removal of water and extractives from softwood with supercritical carbon dioxide," *Industrial and Engineering Chemistry Research* 58, 3170-3174. DOI: 10.1021/acs.iecr.8b05939

Banerjee, S., Sastri, B., Aggarwal, S., and Hakovirta, M. (2022). "Dewatering coal with supercritical carbon dioxide," *International Journal of Coal Preparation and Utilization* 42(5), 1393-1399. DOI: 10.1080/19392699.2020.1715962

Behr, V. C., Hill, S. J., Meder, R., Sandquist, D., Hindmarsh, J. P., Franich, R. A., and Newman, R. H. (2014). "Carbon-13 NMR chemical-shift imaging study of dewatering of green sapwood by cycling carbon dioxide between the supercritical fluid and gas phases," *Journal of Supercritical Fluids* 95, 535-540. DOI: 10.1016/j.supflu.2014.08.026

Cao, M. D., Zhang, X. X., Ren, W. T., Zhu, J. W., Wang, H. K., Xu, H. C., and Yu, Y. (2021). "Effect of drying methods on the cell wall pore structure of *Phyllostachys edulis*," *Journal of Forestry Engineering* 6(6), 58-65. DOI:10.13360/j.issn.2096-1359.202103014

Carignato, A., De, Moraes. C. B., Zimback, L., and Mori, E. S. (2018). "Genetic resistance to rust of *Eucalyptus urophylla* progenies," *Floresta e Ambiente* 25(1), article no. e00094014. DOI: 10.1590/2179-8087.094014

Chen, Y., and Zhu, J. (2019). "Study on bending characteristics of fast growing *Eucalyptus* bookcase shelves by using burgers mode," *Wood Research* 64, 137-144.

Dawson, B. S.W., Pearson, H., Kroese, H. W., and Sargent, R. (2015). "Effect of samples dimension and pre-heating temperature on supercritical CO_2 dewatering of radiata pine sapwood," *Holzforschung* 69, 421-430. DOI: 10.1515/hf-2014-0055

Dawson, B. S.W., and Pearson, H. (2017). "Effect of supercritical CO_2 dewatering

followed by oven-drying of softwood and hardwood timbers," *Wood Science and Technology.* 51, 771-784. DOI: 10.1007/s00226-017-0895-8
Dawson, B. S. W., Pearson, H., Kimberley, M. O., Davy, B., and Dickson, A. R. (2020). "Effect of supercritical CO_2 treatment and kiln drying on collapse in *Eucalyptus nitens* wood," *European Journal of Wood and Wood Products* 78, 209-217. DOI: 10.1007/s00107-020-01500-5
Ferrentino, G., Morozova, K., Mosibo, O. K., Ramezani, M., and Scampicchio, M. (2018). "Biorecovery of antioxidants from apple pomace by supercritical fluid extraction," *Journal of Cleaner Production* 186, 253-261. DOI: 10.1016/j.jclepro.2018.03.165
Franich, R. A., Meder, R., and Behr, V. C. (2020). "Dewatering green sapwood using carbon dioxide undergoing cyclical phase change between supercritical fluid and gas," *Molecules* 25(22), 5367. DOI: 10.3390/molecules25225367
Franich, R. A., Gallagher, S., and Kroese, H. (2014). "Dewatering green sapwood using carbon dioxide cycled between supercritical fluid and gas phase," *The Journal of Supercritical Fluids* 89, 113-118. DOI: 10.1016/j.supflu.2014.02.019
Franich, R. A., Meder, R., and Behr, V. C. (2020). "Dewatering green sapwood using carbon dioxide undergoing cyclical phase change between supercritical fluid and gas," *Molecules* 25(22), 5367. DOI: 10.3390/molecules25225367
Gabitov, R. F., Khairutdinov, V. F., Gumerov, F. M., and Gabitov, F. R. (2017). "Drying and impregnation of wood with propiconazole using supercritical carbon dioxide," *Russian Journal of Physical Chemistry B* 11, 1223-1230. DOI: 10.1134/S1990793117080048
GB/T 1931 (2009). "Method for determination of moisture content of wood," Standardization Administration of China, Beijing, China.
GB/T 6491 (2012). "Drying quality of sawn timber," Standardization Administration of China, Beijing, China.
Hayashi, K., and Terazawa, S. (1975). "Studies on cell collapse of water saturated balsa wood, 3: The effect of the tensile stress on the collapse intensity," *Mokuzai Gakkaishi* 21(5), 278-282.
Huang, C., Chui, Y.H., Gong, M., and Chana, F. (2020). "Mechanical behavior of wood compressed in radial direction: Part II. Influence of temperature and moisture content," *Journal of Bioresources and Bioproducts* 5(4), 266-275. DOI:10.1016/j.jobab.2020.10.005
Meder, R., Franich, R. A., Callaghan, P. T., and Behr, V. C. (2015). "A comparative study of dewatering of *Pinus radiata* sapwood using supercritical CO_2 and conventional forced air-drying via in situ magnetic resonance microimaging (MRI)," *Holzforschung* 69, 1137-1142. DOI: 10.1515/hf-2014-0134
Morales, P., Gentina, J. C., Aroca, G., and Mussatto, S. I. (2017). "Development of an acetic acid tolerant *Spathaspora passalidarum* strain through evolutionary engineering with resistance to inhibitors compounds of autohydrolysate of *Eucalyptus globulus*," *Industrial Crops and Products* 106, 5-11. DOI:10.1016/j.indcrop.2016.12.023
Newman, R. H., Franich, R. A., Meder, R., Hill, S. J., Kroese, H., Sandquist, D., Hindmarsh, J. P., Schmid, M. W., Fuchs, J., and Behr, V. C. (2016). "Proton

magnetic resonance imaging used to investigate dewatering of green sapwood by cycling carbon dioxide between supercritical fluid and gas phase," *The Journal of Supercritical Fluids* 111, 36-42. DOI: 10.1016/j.supflu.2016.01.007
Pang, X. N., Yang, X., Li, X. J., Cao, M., and Yang, X. (2021). "Improvement of porosity and dye permeability of moso bamboo splints by alkali etching," *Journal of Forestry Engineering* 6(6), 44-50. DOI:10.13360/j.issn.2096-1359.202012030
Ruben, A. A., Victor, S.V., Nayalia, P. P., and Jose, T. M. (2020). "Radio frequency vacuum drying of *Eucalyptus nitens* juvenile wood," *BioResources* 15(3), 4886-4897.DOI: 10.15376/biores.15.3.4886-4897
Teixeira, T. O. B., Silva, M. L., Jacovine, L. A. G., Valverde, S. R., Silva, J. C., and Pires, V. A. V. (2009). "The perception of manufacturers of the furniture center of Uba-MG about the use of *Eucalyptus* wood," *Revista Arvore.* 33(5), 969-975. DOI: 10.1590/S0100-67622009000500019
Tiemann, H. D. (1941). "Collapse in wood as shown by microscope," *Journal of Forestry* 39 (3), 271-282. DOI: 10.1093/jof/39.3.271
Todd, R., and Baroutian, S. (2017). "A techno-economic comparison of subcritical water, supercritical CO_2 and organic solvent extraction of bioactives from grape marc," *Journal of Cleaner Production* 158, 349-358. DOI: 10.1016/j.jclepro.2017.05.043
Wingate-Hill, R., and Cunningham, R. B. (1986). "Compression drying of sapwood," *Wood & Fiber Science* 18, 315-326.
Xu, W., Chen, P., Yang, Y., Wang, X., and Liu, X. (2021). "Effects of freezing and steam treatments on the permeability of *Populus tomentosa*," ["Einfluss von Vereisungs-und Dampfbehandlung auf die Permeabilitat von *Populus tomentosa*"], *Materialwissenschaft und Werkstofftechink* 52(8), 907-915. DOI:10.1002/mawe.202000227
Yang, L., Han, T. Q., and Fu, Y. D. (2020). "Effect of heat treatment and wax impregnation on dimensional stability of *Pterocarpus macrocarpus* wood," *Wood Research* 65(6), 963-974.
Yang, L., and Liu, H. H. (2020). "Effect of supercritical CO_2 drying on moisture transfer and wood property of *Eucalyptus urophydis*," *Forests* 11(10), article no. 1115. DOI: 10.3390/f11101115
Yang, L. (2021). "Effect of temperature and pressure of supercritical CO_2 on dewatering, shrinkage and stresses of *Eucalyptus* wood," *Applied Sciences* 11(18), 8730. DOI:10.3390/APP11188730
Yang, L., and Jin, H. H. (2021). "Effect of heat treatment on the physic-mechanical characteristics of *Eucalyptus urophylla* S.T. Blake," *Materials* 14(21), 6643. DOI: 10.3390/MA14216643
Yang, Y. Q., Xu, W., Liu, X., and Wang, X. D. (2021) "Study on permeability of *Cunninghamia lanceolata* based on steam treatment and freeze treatment," *Wood Research* 66(5), 721-731. DOI: 10.37763/wr.1336-4561/66.5.721731
Yang, L., Zheng, J. T., and Huang, N. (2022). "The characteristics of moisture and shrinkage of *Eucalyptus urophylla* × *E. grandis* wood during conventional drying," *Materials* 15(9), article no. 3386. DOI: 10.3390/MA15093386
Zhang, Y. L., Miao, P., Zhuang, S. Z., Wang, X. M., Xia, J. W., and Wu, L. M. (2011). "Improving the dry-ability of *Eucalyptus* by pre-microwave or pre-freezing

treatment," *Journal of Nanjing Forestry University (Natural Science Edition)* 35(2), 61-64. DOI: 10.3969 /j.issn.1000- 2006.2011.02.013
Zhang, J. W., J, H.H. and Yang, L. (2019). "Application of supercritical CO_2 fluid to wood drying," *World Forestry Research* 32(6), 37-42. DOI: 10.13348/j.cnki.sjlyyj.2019.0052.y
Zhang, J. W., Liu, H. H., Yang, H., and Yang, L. (2020). "Drying characteristics of *Eucalyptus urophylla* × *E. grandis* with supercritical CO_2," *Materials* 13, article no. 3989. DOI: 10.3390/ma13183989
Zhang, L., Chen, Z. H., Dong, H. R., Fu, S., Ma, L., and Yang, X. J. (2021). "Wood plastic composites based wood walls structure and thermal insulation performance," *Journal of Bioresources and Bioproducts* 6(1), 65-74. DOI: 10.1016/J.JOBAB.2021.01.005
Zhao, X. Y., Huang, Y. J., Fu, H. Y., Wang, Y. L., Wang, Z., and Sayed, U. (2021). "Deflection test and modal analysis of lightweight timber floors," *Journal of Bioresources and Bioproducts* 6(3), 266-278. DOI: 10.1016/j.jobab.2021.03.004
Zhen, X., Deng, Y., LI, Y. Z., and Zhu, X. M. (2021). "Design and experiment of pruning machine for eucalyptus trees," *Journal of Forestry Engineering* 6(2), 148-156. DOI:10.13360/j.issn.2096-1359.202004026
Zhou, Y. D., Fu, F., Li, X. J., Jiang, X. M., and Chen, Z. L. (2009). "Effects of microwave treatment on residue growth stress and microstructure of *Eucalyptus urophylla*," *Journal of Beijing Forestry University* 31(2), 146-150. DOI: 10.13332/j.1000-1522. 2009.02.023
Zuo, C. L., Cao, Y. J., and Zhou, Y. (2016). "A review of formation mechanism and control of collapse in *Eucalyptus* wood," *World Forestry Research* 29(1), 58-63. DOI: 10.13348 /j.cnki.sjlyyj.2016.01.007

Article submitted: June 2, 2022; Peer review completed: June 29, 2022; Revisions accepted: July 1, 2022; Published: July 14, 2022.
DOI: 10.15376/biores.17.3.5116-5128